Lipid Intermediates in Membrane Fusion: Formation, Structure, and Decay of Hemifusion Diaphragm

Yonathan Kozlovsky,* Leonid V. Chernomordik,† and Michael M. Kozlov*

*Department of Physiology and Pharmacology, Sackler Faculty of Medicine, Tel Aviv University, Tel Aviv 69978, Israel; and †Section on Membrane Biology, The Laboratory of Cellular and Molecular Biophysics, National Institute of Child Health and Human Development, National Institutes of Health, Bethesda, Maryland 20892-1855 USA

ABSTRACT Lipid bilayer fusion is thought to involve formation of a local hemifusion connection, referred to as a fusion stalk. The subsequent fusion stages leading to the opening of a fusion pore remain unknown. The earliest fusion pore could represent a bilayer connection between the membranes and could be formed directly from the stalk. Alternatively, fusion pore can form in a single bilayer, referred to as hemifusion diaphragm (HD), generated by stalk expansion. To analyze the plausibility of stalk expansion, we studied the pathway of hemifusion theoretically, using a recently developed elastic model. We show that the stalk has a tendency to expand into an HD for lipids with sufficiently negative spontaneous splay, $\tilde{J}_s < 0$. For different experimentally relevant membrane configurations we find two characteristic values of the spontaneous splay. $\tilde{J}_s^*$ and $\tilde{J}_s^{**}$, determining HD dimension. The HD is predicted to have a finite equilibrium radius provided that the spontaneous splay is in the range $\tilde{J}_s^{**} < \tilde{J}_s < \tilde{J}_s^*$, and to expand infinitely for $\tilde{J}_s < \tilde{J}_s^{**}$. In the case of common lipids, which do not fuse spontaneously, an HD forms only under action of an external force pulling the diaphragm rim apart. We calculate the dependence of the HD radius on this force. To address the mechanism of fusion pore formation, we analyze the distribution of the lateral tension emerging in the HD due to the establishment of lateral equilibrium between the deformed and relaxed portions of lipid monolayers. We show that this tension concentrates along the HD rim and reaches high values sufficient to rupture the bilayer and form the fusion pore. Our analysis supports the hypothesis that transition from a hemifusion to a fusion pore involves radial expansion of the stalk.

INTRODUCTION

Fusion of two membranes into one is a stage common to diverse cell biological processes. It remains to be understood whether different fusion reactions proceed via similar intermediates and are driven by similar forces (Chernomordik et al., 1995b; Jahn and Sudhof, 1999). A large class of fusion reactions apparently involve hemifusion, i.e., joining of the apposing, contacting lipid monolayers (Fig. 1, *b-d*) of the two membranes prior to a merger of two other, distal monolayers (Chernomordik et al., 1987, 1995a,b, 1997, 1998; Ellens et al., 1985; Gaudin et al., 1999; Helm et al., 1989; Hui et al., 1981; Kemble et al., 1994; Lee and Lentz, 1997; Melikyan et al., 1995, 1997; Pantazatos and MacDonald, 1999; Song et al. 1991). Thus, hemifusion precedes formation of an aqueous connection between membrane contents referred to as a fusion pore. While widely considered to be a key stage in membrane fusion ((Jahn and Sudhof, 1999), but see Lindau and Almers, 1995; Peters et al., 2001), hemifusion is poorly understood both on the structural level and in terms of the physical forces involved. The goal of the present work is to analyze theoretically the pathways of the intermediate membrane structures emerging in the course of hemifusion and the forces driving evolution of these intermediates into a fusion pore.

Hemifusion is thought to start with formation of a stalk, a local connection between the contacting monolayers of two membranes (Gingell and Ginsberg, 1978; Kozlov and Markin, 1983). Further evolution of the hemifusion intermediate and the mechanism of its transition into a fusion pore remains unknown. The transition can proceed by one of the three following scenarios. The first model, named the stalk-pore hypothesis (Chernomordik et al., 1995b, 1987; Kozlov et al., 1989), suggests that the stalk (Fig. 1 *b*) expands radially and brings the distal monolayers of the two membranes together into a single bilayer. The resulting structure (Fig. 1 *c*) is referred to as a hemifusion diaphragm (HD). Opening of a fusion pore (Fig. 1 *e*) within the HD completes the fusion reaction. To allow formation of the pore rim, the radius of the diaphragm has to exceed a certain value approximately equal to the lipid monolayer thickness. In the second model, the fusion pore forms directly from the stalk and constitutes from the very beginning a bilayer connection between the membranes (Kuzmin et al., 2001; Siegel, 1993). The third type of models is based on the Brownian dynamics and Monte Carlo simulations of bilayer fusion (Muller et al., 2002; Noguchi and Takasu, 2001a,b). It has been proposed that the stalk undergoes anisotropic rather than radial growth and forms elongated connections between the contacting monolayers of the membranes (Fig. 1 *d*) (Muller et al., 2002). The stalk destabilizes the contacting bilayers and promotes the formation of holes next to it in each of the two fusing membranes. The rims of the two holes then merge to produce an intermembrane bilayer connection, a fusion pore. Note that out of these three models only the stalk-pore hypothesis suggests that the

Submitted March 14, 2002, and accepted for publication June 12, 2002.

Address reprint requests to Michael M. Kozlov, Department of Physiology and Pharmacology, Sackler Faculty of Medicine, Tel Aviv University, Tel Aviv 69978, Israel. Tel.: 972-3-640-7863; Fax: 972-3-640-9113; E-mail: michk@post.tau.ac.il.

0006-3495/02/11/2634/18 $2.00

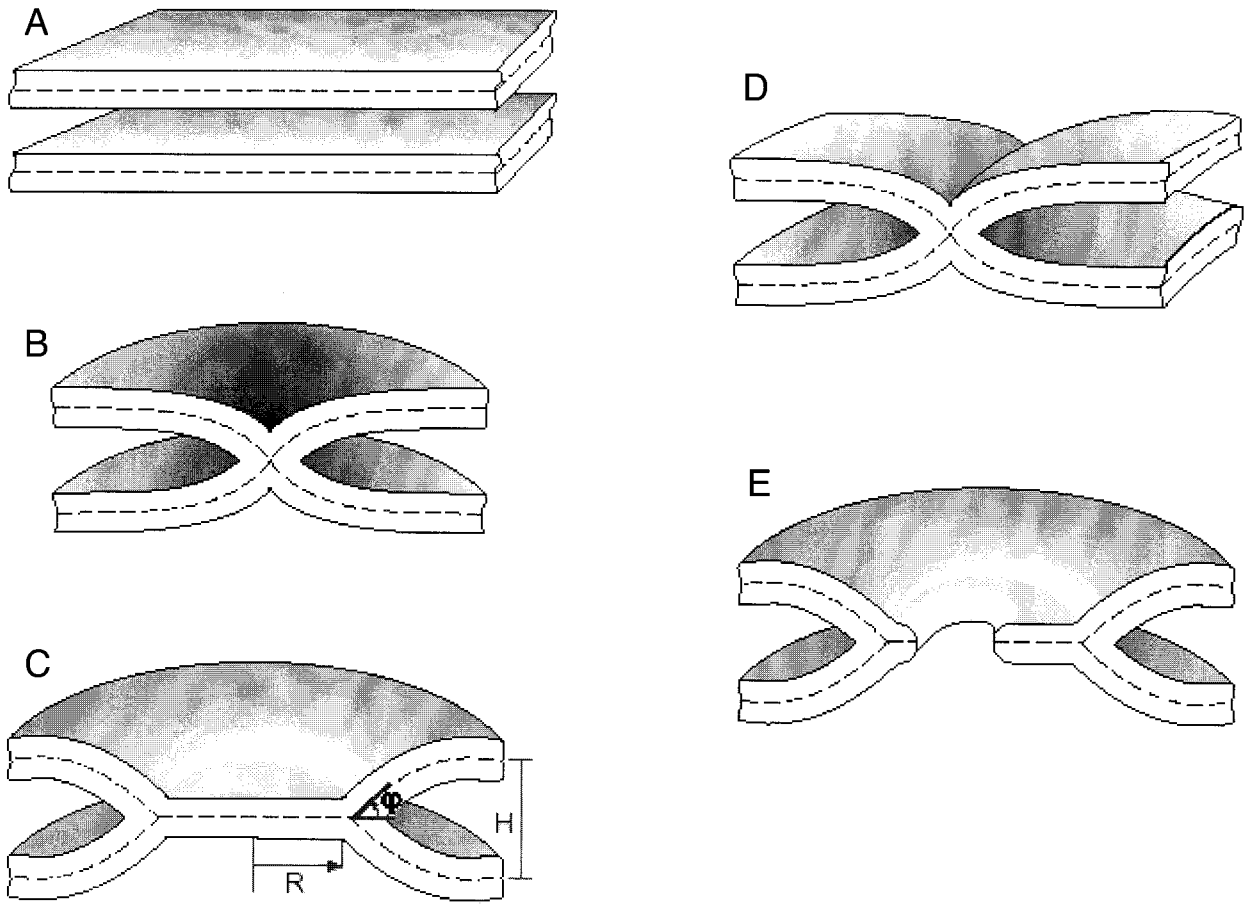

FIGURE 1 Pathway of membrane fusion. (*a*) Initial flat membranes. (*b*) Fusion stalk. (*c*) Circular hemifusion diaphragm. (*d*) Elongated connection. (*e*) Fusion pore.

fusion pore opens in a single bilayer (HD) and involves only the lipids of the distal monolayers of the fusing membranes.

The choice among these three models boils down to two questions: 1) the dependence of fusion pore formation on the composition of different membrane monolayers and 2) the existence and possible size of the HD. The effects of the lipid composition of the distal monolayers are consistent with the stalk-pore hypothesis. In particular, modifying the distal membrane monolayers with lysophosphatidylcholine (LPC), a lipid that promotes pore formation in a single bilayer (Chernomordik et al., 1985), or with the pore-forming amphiphile chlorpromazine, facilitates transition from a hemifusion to a fusion pore (Chernomordik et al., 1995a,b, 1998; Grote et al., 2000; Melikyan et al., 1997). Estimates of the possible dimensions of the hemifusion intermediates differ dramatically depending on the experimental systems. They can have macroscopic sizes for structures described in fusion of two planar bilayers (Chernomordik et al., 1987) or for influenza hemagglutinin (HA)-mediated fusion between cell and planar bilayer (Melikyan et al., 1995). On the other hand, hemifusion intermediates in exocytosis (Chandler and Heuser, 1980; Olbricht, 1984; Ornberg and Reese, 1981) and in HA-mediated fusion between cells (Frolov et al., 2000) are too small to be detected (less than a few tens of nanometers in diameter). This discrepancy can reflect differences in the lateral tension driving expansion of the fusion stalk and/or the problems of detection of labile hemifusion intermediates. In brief, the data on the sizes of the hemifusion intermediate remain inconclusive.

Given the absence of direct experimental evidence for or against the existence of HDs, the theoretical analysis of the structure and energy of hemifusion intermediates and the conditions of their progression to a fusion pore acquires critical importance.

Hemifusion structures have been analyzed using the elastic models inspired by the strongly curved shapes of the monolayers forming the fusion stalks and the rims of the HDs. The models are based on the theory of bending elasticity of membrane monolayers (Helfrich, 1973), whose major concept is the monolayer spontaneous curvature, J_s, characterizing the intrinsic tendency of the monolayer to adopt a bent shape. The structure and energy of the fusion stalk have been modeled in a series of works over the last two decades (Kozlov et al., 1989; Kozlov and Markin, 1983;

Kozlovsky and Kozlov, 2002; Kuzmin et al., 2001; Leikin et al., 1987; Markin and Albanesi, 2002; Markin et al., 1984; Siegel, 1993, 1999). The early model predicted formation of a large and even infinitely expanding HD for tension-free membranes with contacting monolayers of a sufficiently strong negative spontaneous curvature (Chernomordik et al., 1995b; Kozlov and Markin, 1983). Further analysis (Siegel, 1993, 1999) took into account, in addition to the effects of membrane bending, the energy of the structural defects referred to as hydrophobic interstices, which unavoidably emerge inside the hemifusion intermediates (see Fig. 11 *a*). For almost all feasible values of the spontaneous curvature radial expansion of the stalk in this modified stalk model stops prior to the formation of a hemifusion diaphragm with radius greater than or equal to the monolayer thickness. Even for very negative values of J_s corresponding to the transition of phosphatidylethanolamine (DOPE) from lamellar (*L*) to inverted hexagonal (*HII*) phase the diaphragm was predicted to have a very slight tendency to expand (Siegel, 1999). It was proposed that in most cases transition of the fusion stalk into a fusion pore proceeds directly from local intermediate referred to as *trans*monolayer contact (Siegel, 1993, 1999). However, these results were based on specific assumptions about the structure of the fusion intermediates, which yielded extraordinarily large energy of the initial stalk and led to the formulation of the "energy crisis" of the model. These assumptions had to be corrected to demonstrate that stalk formation is feasible within a realistic time span (Kuzmin et al., 2001; Kozlovsky and Kozlov, 2002; Markin and Albanesi, 2002). The possible effects of this correction on the important conclusion that stalk expansion into an HD is energetically unfavorable have not been analyzed.

To summarize, both experimental and theoretical studies left open the question of the fusion pathway downstream from stalk formation.

Goal of the present work

The aim of this study is to answer theoretically the following questions: Is expansion of the stalk favorable energetically for any reasonable lipid composition of the membranes? What kind of stalk expansion is more favorable, the radial one leading to an HD or the linear one resulting in an elongated connection? In case the lipid composition does not favor spontaneous HD expansion, what force has to be generated by the specialized proteins such as HA, referred to as the fusion proteins, to drive this process? What factor drives nucleation of the fusion pore within the hemifusion intermediate?

Our theory predicts expansion of the fusion stalk into an HD for lipids characterized by a sufficiently negative spontaneous curvature. Radial expansion of the stalk is found to be more favorable energetically than linear expansion in all practically important cases. For the lipids that do not form an HD spontaneously, we analyze a force that can drive this process and show that this force can be generated by the fusion proteins. We show that the portions of the monolayers close to the rim of an HD are subject to very high lateral tension and suggest that this tension drives the formation of the fusion pore.

MODEL OF HEMIFUSION INTERMEDIATES

Structures of hemifusion intermediates

We consider hemifusion of two flat lipid bilayers, which in the initial state are parallel to each other (Fig. 1 *a*). The structure of the initial hemifusion intermediate, the fusion stalk, illustrated in Fig. 1 *b*, has been suggested and discussed in detail recently (Kozlovsky and Kozlov, 2002). We sketch its major properties in Appendix A.

Here, we consider the intermediates, which result directly from an expansion of the fusion stalk. The radial expansion leads to a flat circular diaphragm formed by the distal monolayers of the two membranes, which is bounded by the expanded stalk (Fig. 1 *c*). Strictly speaking, only the flat bilayer portion represents the HD *per se*. However, we will use a looser terminology and refer to the whole structure including the diaphragm itself and the expanded stalk as the HD. We assume that the HD retains the major structural features of the initial stalk (Appendix A). Specifically, the hydrophobic interstice, which otherwise emerges along the rim of the diaphragm, is filled because of the tilt and the related stretching (Hamm and Kozlov, 2000) of the hydrocarbon chains. The tilt decays from the diaphragm rim along the monolayers of all three joined bilayers (see Fig. 12). As a result, the profiles of the monolayers form sharp corners in front of the diaphragm rim, and the overall membrane deformation is a superposition of the tilt of the hydrocarbon chains and the bending of the monolayer surfaces.

The linear expansion of the stalk gives rise to the elongated connection, whose cross-section is identical to that of the initial stalk (Fig. 1 *d*) and whose ends are bound by half stalks.

Constraints on the HD configurations

The shape of the expanded stalk bounding the HD rim is, usually, constrained. In most cases, the two membranes connected by the stalk wings to the diaphragm rim are maintained flat and parallel. We define the inter-membrane distance H as the spacing between the midplanes of the parallel membranes (Fig. 1 *c* and 2 *a* and *b*). Whereas matching of the expanded stalk to a certain value of H provides a common constraint, additional restrictions on the shapes of the stalk wings can be related to specific features of membrane configurations. We consider two types of constraints, which are relevant experimentally (Fig. 2).

The first configuration illustrated in Fig. 2 *a* models a membrane contact mediated by fusion proteins. We take the intermembrane distance to have a typical value of $H = 13$ nm (Monck and Fernandez, 1992; Skehel and Wiley, 2000). The fusion proteins situated next to the diaphragm and connecting the two parallel membranes restrict the radial distance r between the diaphragm rim and the place where the expanded stalk is connected to the flat part of the membranes (Fig. 2 *a*). This distance will be referred to as the stalk width, r. Dependence of the energy of the initial stalk on the value of r has been examined in Kozlovsky and Kozlov (2002). Based on these results we take $r = 25$ nm, which corresponds to the range where the initial stalk energy depends weakly on this parameter. In addition, we verify the sensitivity of the HD energy to r.

The second membrane configuration illustrated in (Fig. 2 *b*) is a stack of pure lipid bilayers constituting a lamellar (*L*) phase (Rand and Parsegian, 1989). Provided that the membrane surfaces do not carry electric charge, the intermembrane distance resulting from a balance of the membrane

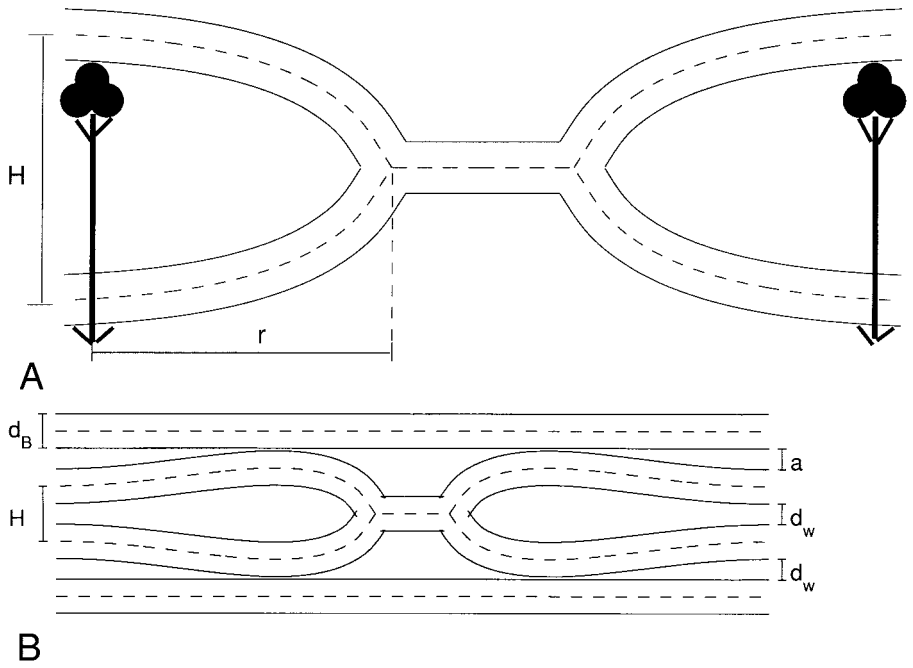

FIGURE 2 Restrictions of HD configurations. (*a*) Limitations of the width of the expanded stalk by fusion proteins. (*b*) Limitations of the amplitude of the wave-like shape of the expanded stalk by the adjacent bilayers in a lamellar phase.

interactions is $H \approx 6.4$ nm, what corresponds to thickness of water layer between the adjacent membranes of about $d_w \approx 2.4$ nm (Rand and Parsegian, 1989). In this system, as it follows from the computations below, the wings of the expanded stalk have a shape of a wave with amplitude a (Fig. 2 *b*). The membranes, which are situated within the stack just above and below the fusion site, restrict the amplitude a. As a result the latter cannot exceed a certain value, $a \leq H - d_B$, in which d_B is the bilayer thickness (Fig. 2 *b*). Taking into account that $d_B = 4$ nm, the amplitude of the wings should be $a \leq 2.4$ nm.

Elastic model

Below, we compute the dependence of the energy of the HD and the elongated connection on their dimensions. Our theoretical tool is the elastic theory of tilt and splay of lipid monolayers (Hamm and Kozlov 1998, 2000, 2002; May, 2000), which is sketched in Appendix B. The major structural characteristic of lipids is the spontaneous splay of the hydrocarbon chains, $\tilde{J}_s$, introduced originally as the spontaneous curvature (Helfrich, 1973). The spontaneous splay is determined by the relative dimensions of the polar heads and the hydrocarbon moieties of lipid molecules and changes from positive values for lysolipids, such as $\tilde{J}_s^{LPC} \approx 1/3.8\ \text{nm}^{-1} = 0.26\ \text{nm}^{-1}$ for LPC (Fuller, 2001), through slightly negative values for common bilayer-forming lipids, such as $\tilde{J}_s^{DOPC} \approx -1/8.7\ \text{nm}^{-1} = -0.11\ \text{nm}^{-1}$ for dioleoylphosphatidylcholine (DOPC) (Chen and Rand, 1997), and down to strongly negative values, such as $\tilde{J}_s^{DOPE} \approx -1/2.8\ \text{nm}^{-1} = -0.35\ \text{nm}^{-1}$ for DOPE (Kozlov et al., 1994; Leikin et al., 1996; Rand and Fuller, 1994). The elastic properties of lipids are characterized by the monolayer splay modulus, κ, introduced originally as the bending modulus (Helfrich, 1973) and having the value $\kappa \approx 4 \times 10^{-20}\ J$ (Niggemann and others 1995) and by the tilt modulus, κ_t, estimated as $\kappa_t \approx 40$ mN/m (Hamm and Kozlov, 1998, 2000; May, 2000). The details of the elastic model and its mathematical presentation are given in Appendix B.

Outline of analysis

We characterize the configuration of the HD by several parameters. The dimension of the diaphragm is determined by its radius, R (Fig. 1 *c*). The diaphragm rim is bounded by the expanded stalk. The junction of three bilayers along the diaphragm rim is characterized in each monolayer by the angle ϕ of tilt of the hydrocarbon chains with respect to the monolayer surface, and the angle φ between the midplane of the diaphragm and that of the membrane of the expanded stalk (Fig. 1 *c*). The illustration of the tilt angles and discussion of their relationships with φ are presented in the Appendix C.

The constraints imposed on the expanded stalk result in membrane energy additional to that related to the diaphragm *per se*. Therefore, we first consider an "ideal" case where the expanded stalk is unconstrained and its membrane is free to adopt a shape of minimal elastic energy. In this case, determination of the configuration and the energy of an HD of radius R includes the following steps. First, for given value of the angle φ, the elastic energy (Appendix B) is integrated over all monolayers of the structure (Fig. 1 *c*). The result is minimized with respect to 1) the shape of the wings of expanded stalk and 2) the distribution of the chain tilt over the monolayer surfaces. The values of the tilt angles in the junction, α, β, and γ, (see Fig. 13) are determined by their relationship with φ (Appendix C). The computations are performed numerically by the Method of Finite Elements, which is equivalent to solving the Euler-Lagrange equations. Second, the procedure below is repeated for different values of φ and the energy is minimized with respect to this parameter as well.

At the next step we perform these computations for the two constrained membrane systems accounting for the limitations of the shape of the expanded stalk mentioned above. The same calculation procedure above is easily adapted for analysis of the conformation and energy of the elongated connection (Fig. 1 *d*) by accounting for its geometry. Specifically, the angle φ and the tilt angles of the contacting, ϕ_c, and the distal, ϕ_d, monolayers at the junction point do not come into play as minimization parameters. They are fixed at $\pi/4$ for the following reason. As it follows from Fig. 1 *d*, the angle φ is equal in this case to tilt angle of the distal monolayer, $\varphi = \phi_d$. The sum of the tilt angles of the two monolayers is fixed, $\phi_d + \phi_c = \pi/2$. On the other hand, we limit our consideration by small deformations (Appendix B), what requires $|\bar{t}| = |tg\phi| \leq 1$, meaning $|\phi| \leq \pi/4$. To satisfy this limitation we have to adopt for the elongated connection $\varphi = \phi_c = \phi_d = \pi/4$.

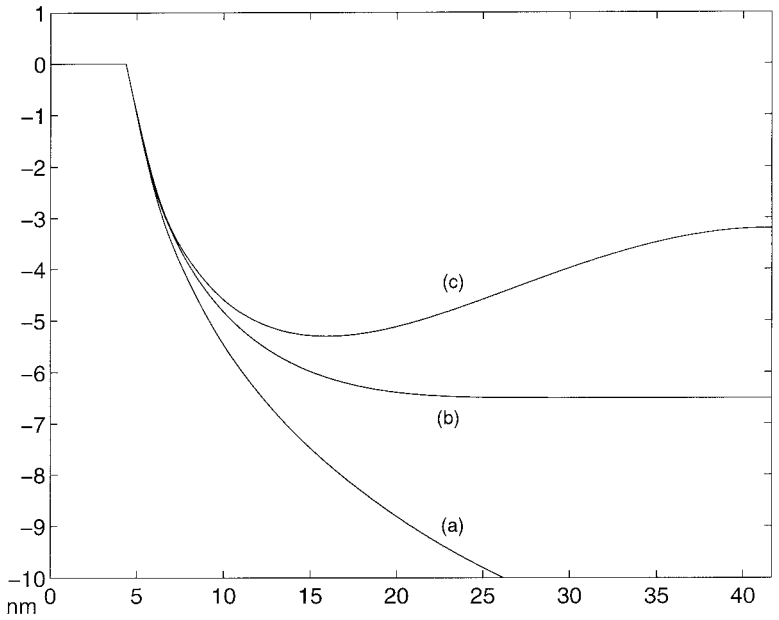

FIGURE 3 Profile of HD for (*a*) unconstraint HD, (*b*) the intermembrane distance $H = 13$ nm, and the stalk width $r = 25$ nm, (*c*) the intermembrane distance $H = 6.4$ nm, and the amplitude of the wave-like shape of the expanded stalk $a = 2.4$ nm.

To verify whether expansion of the stalk can be favorable for any reasonable membrane composition, we perform the calculation for different spontaneous splays of the membrane monolayers.

RESULTS

Configuration of HD

First, we determined the structure of HD for symmetric membranes with monolayers of equal spontaneous splay, $\tilde{J}_s$. The qualitative character of the shape of the expanded stalk bounding the HD rim and of the tilt distribution in the HD monolayers turned out to be largely insensitive to $\tilde{J}_s$ and the diaphragm radius R. The profiles of HD shape represented by quarter of HD cross-section are illustrated in Fig. 3 for $\tilde{J}_s = -0.1$ nm^{-1} and $R = 4$ nm.

In case of an unconstrained HD illustrated in Fig. 3 *a*, the expanded stalk far from the diaphragm rim adopts a shape of vanishing mean curvature, which is called catenoid—the axisymmetric minimal surface (Nitsche, 1989).

For the case where the intermembrane distance and the width of the expanded stalk are constrained by $H = 13$ nm and $r = 25$ nm, respectively, the HD configuration is presented in Fig. 3 *b*.

For the small intermembrane distance, $H = 6.4$ nm, and the amplitude of the wings of the expanded stalk equal to $a = 2.4$ nm the HD profile is illustrated in Fig. 3 *c*.

Energy of HD

The energy of HD as a function of its radius, $F(R)$, is illustrated in Fig. 4 for different values of $\tilde{J}_s$. The intercepts of the curves in Fig. 4 represent the energy of the initial stalks and correspond to the results of the previous work (Kozlovsky and Kozlov, 2002).

The solid lines (Fig. 4) illustrate the energy of the unconstrained HD. If $\tilde{J}_s$ is not sufficiently negative, expansion of the HD results in monotonically increasing energy (Fig. 4 *a*). For more negative spontaneous splay, $\tilde{J}_s \leq -0.2$ nm^{-1}, the slope of $F(R)$ becomes negative for small diaphragm radii so that the energy of HD starts to decrease with R (Fig. 4 *b*). This means that a stalk tends to expand into an HD. However, this expansion is limited. Indeed, the energy $F(R)$ changes nonmonotonically with R and adopts, as illustrated in Fig. 4 *b*, a minimal value at a certain R^* referred to as the equilibrium HD radius. For even more negative spontaneous splay, $\tilde{J}_s \leq -0.27$ nm^{-1}, the energy $F(R)$ decreases monotonically with R, and the HD tends to expand without limit.

The HD energies $F(R)$ for the intermembrane distances $H = 13$ nm and the width of the expanded stalk restricted by $r = 25$ nm are represented in Fig. 4 by the dashed lines. Numerical analysis has shown that $F(R)$ is rather insensitive to the specific value of r. However, if the latter becomes very large, $r \to \infty$, the energy of the HD approaches the energy of an unconstrained HD.

The energies corresponding to $H = 6.4$ nm are shown in Fig. 4 by dotted lines. According to our analysis, the amplitude of the stalk wings in this case tends to grow, thus, decreasing the energy. As mentioned above, this growth is restricted by the adjacent membranes in the multilamellar phase so that the energies represented in Fig. 4 correspond to $a = 2.4$ nm.

The reason for different behavior of the function, $F(R)$, determined by the spontaneous splay, $\tilde{J}_s$, is related to de-

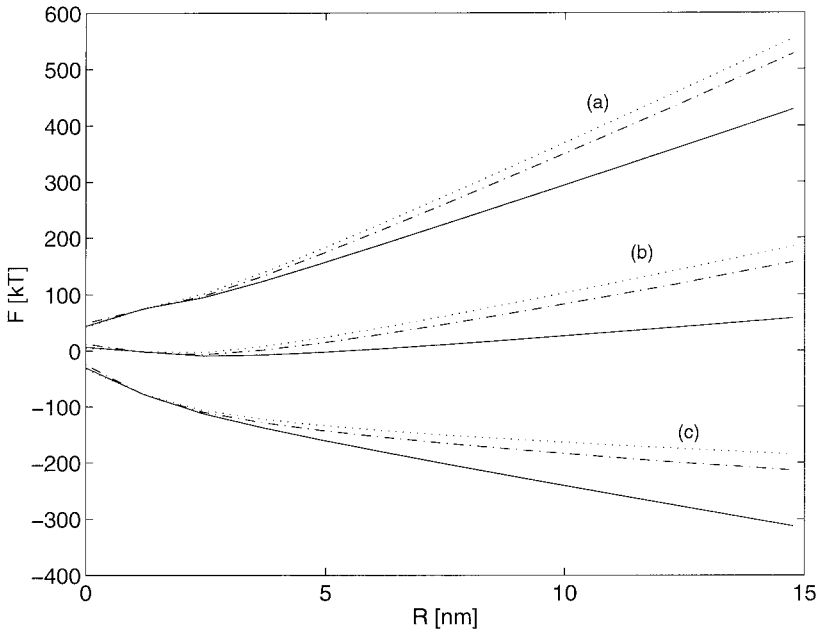

FIGURE 4 Dependence of the energy of a hemifusion diaphragm on its radius for different values of intermembrane distance, H, and different spontaneous splay of membrane monolayers, $\tilde{J}_s$. Solid curves, unconstrained HD; dashed curves, $H = 13$ nm; dotted curves, $H = 6.4$ nm. (*a*) $\tilde{J}_s = -0.11$ nm^{-1}; (*b*) $\tilde{J}_s = -0.22$ nm^{-1}; (*c*) $\tilde{J}_s = -0.34$ nm^{-1}.

pendence of the surface density of the elastic energy, f (Appendix B), on the HD radius, R. The total HD energy can by presented as $F = \langle f \rangle \cdot A$, in which A is the area of the deformed parts of the monolayers, and $\langle f \rangle$ is the energy density averaged over A. The slope of $F(R)$ is determined by $dF/dR = \langle f \rangle \cdot dA/dR + A \cdot d\langle f \rangle/dR$.

For large values of R, the area A is proportional to the HD perimeter, and, hence, $A \sim R$, while the average density $\langle f \rangle$ does not depend on the radius, $\langle f \rangle_{R\to\infty} = \text{const}$, so that $d\langle f \rangle/dR = 0$. As a result, the energy F changes linearly with the diaphragm circumference, $F \sim \langle f \rangle_{R\to\infty} \cdot R$, and its slope is constant, $dF/dR|_{R\to\infty} = 2\pi\sigma$. The value σ, which is referred to as the HD line tension, is linear in the spontaneous splay and, according to our numerical computations, is presented by $\sigma = (8 + 30 \cdot \tilde{J}_s)\ kT$/nm, in which kT is the product of the Boltzmann constant and the absolute temperature. According to this equation, the linear tension, σ, and, hence, the slope of $F(R)$ at large diaphragm radii, $R \to \infty$, changes from the positive to the negative values (Fig. 4) at $\tilde{J}_s \approx -0.27$ nm^{-1}.

For small values of the diaphragm radius, the energy density $\langle f \rangle$ changes considerably with R, so that its derivative, $d\langle f \rangle/dR \neq 0$, influences strongly the slope of the function $F(R)$. As follows from our calculations, important contributions to $d\langle f \rangle/dR$ are provided by the terms proportional to the average square tilt, $\langle t^2 \rangle$, and the average square splay, $\langle \tilde{J}^2 \rangle$. It can be shown that $d\langle t^2 \rangle/dR < 0$ and $d\langle \tilde{J}^2 \rangle/dR < 0$. These contributions, which vanish for large R, provide one of the major reasons for the regime where the slope of the total HD energy, dF/dR, whereas being positive for the large HD radii R, is negative for small R, and, hence, the diaphragm has a finite equilibrium radius, R^*.

Equilibrium dimensions of HD

The dependence of the equilibrium HD radius R^* on the spontaneous splay of the membrane monolayers, $\tilde{J}_s$, is presented in Fig. 5 for the unconstrained (Fig. 5 *a*) and the two constrained (Fig. 5 *b* and *c*) HD configurations. Whereas the curves in Fig. 5 are shifted with respect to each other, they have similar qualitative behavior. There are two negative characteristic values of the spontaneous splay, $\tilde{J}_s^*$ and J_s^{**}. HD of a nonvanishing equilibrium radius, R^*, forms when $\tilde{J}_s$ becomes more negative than the first characteristic value, $\tilde{J}_s < \tilde{J}_s^*$, and R^* becomes infinitely large if $\tilde{J}_s$ exceeds the second characteristic negative value, $\tilde{J}_s \leq \tilde{J}_s^{**}$. For the nonconstrained HD, and the intermembrane distances restricted by $H = 13$ nm, the characteristic spontaneous splay adopts the value of $\tilde{J}_s^* \approx -0.19$ nm^{-1}, whereas for $H = 6.4$ nm this value is slightly more negative, $\tilde{J}_s^* = -0.21$ nm^{-1}. The second characteristic spontaneous splay, $\tilde{J}_s^{**}$, equals for the nonconstrained configuration $\tilde{J}_s^{**} = -0.27$ nm^{-1}, whereas for the two constrained configurations it adopts the values of $\tilde{J}_s^{**} \approx -0.31$ nm^{-1} and $\tilde{J}_s^{**} \approx -0.32$ nm^{-1} for $H = 13$ nm and $H = 6.4$ nm, respectively (Fig. 5).

Asymmetric membranes

A question arises as to how sensitive the HD energy is to the spontaneous splay $\tilde{J}_s$ of each of the monolayers, separately. Our analysis shows that for an unconstrained HD the spontaneous splays of the two monolayers equally contribute to the energy. In contrast, constraints of the intermembrane distance H result in asymmetry in contributions of $\tilde{J}_s$ of the two monolayers.

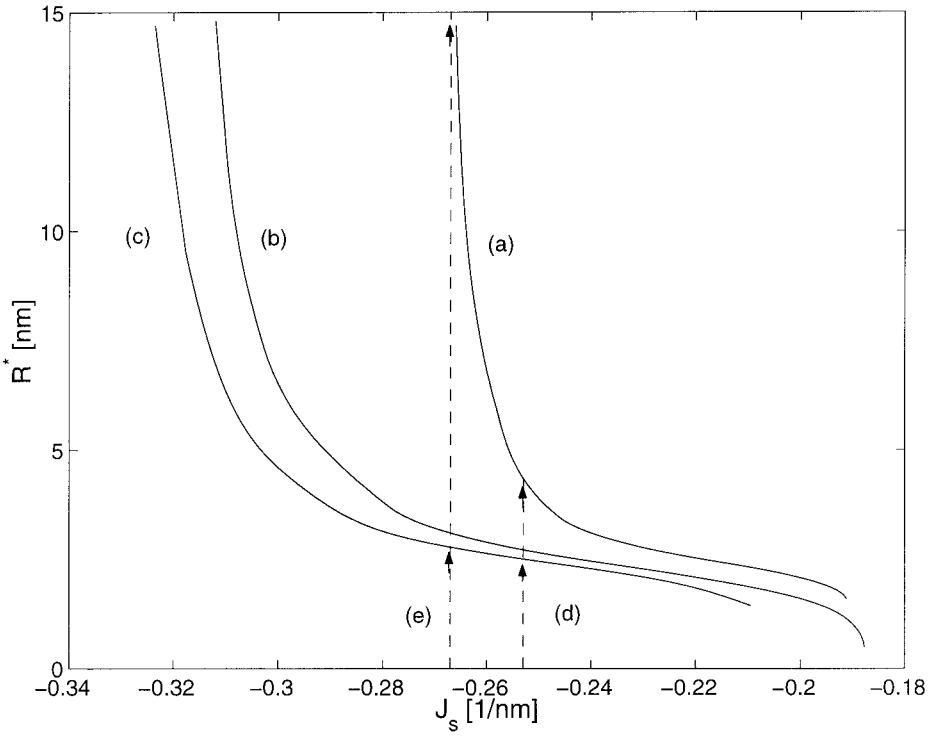

FIGURE 5 Dependence of the equilibrium radius of the hemifusion diaphragm on the spontaneous splay of membrane monolayers. The intermembrane distances are (*a*) unconstrained HD, (*b*) $H =$ 13 nm, and (*c*) $H = 6.4$ nm.

This effect turns out to be insensitive, qualitatively, to the specific values of H and the diaphragm radius R. We illustrate it in Fig. 6 for $R = 3.7$ nm and $H = 13$ nm by representing the dependence of the HD energy on the spontaneous splay for three cases: varying $\tilde{J}_s$ of a symmetric membrane (Fig. 6 *a*); varying the spontaneous splay of the contacting monolayers, $\tilde{J}_s^C$, with the spontaneous splay of the distal monolayers, $\tilde{J}_s^D = -0.11\ \mathrm{nm}^{-1}$ (Fig. 6 *b*); and varying $\tilde{J}_s^D$ with $\tilde{J}_s^C = -0.11\ \mathrm{nm}^{-1}$ (Fig. 6 *c*). According to Fig. 6, the spontaneous splay of the contacting monolayers greatly influ-

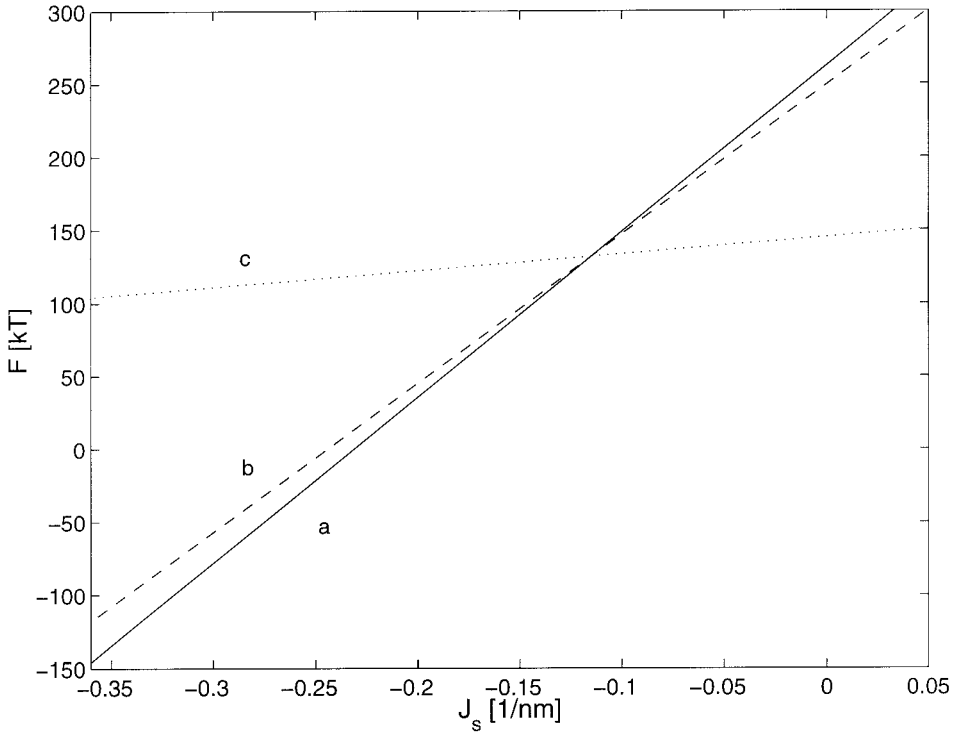

FIGURE 6 Dependence of the energy of hemifusion diaphragm on the spontaneous splay $\tilde{J}_s$ of the two monolayers. The intermembrane distance $H = 13$ nm, the diaphragm radius $R =$ 4 nm, the width of the expanded stalk $r = 25$ nm. (*a*) Case of symmetric membranes; (*b*) $\tilde{J}_s^C$ of the contacting monolayer changes, whereas that of the distal monolayer is fixed, $\tilde{J}_s^D = -0.11\ \mathrm{nm}^{-1}$; (*c*) $\tilde{J}_s^D$ of the distal monolayer changes, whereas that of the contacting monolayer is fixed, $\tilde{J}_s^C = -0.11\ \mathrm{nm}^{-1}$.

ences the energy of the HD, whereas $\tilde{J}_s^D$ of the distal monolayers has practically no effect within the experimentally relevant range of $\tilde{J}_s$. This is in accord with previous results (Kozlovsky and Kozlov, 2002) on the dependence of the stalk energy on the spontaneous splay of the monolayers.

Lateral tensions in HD

The portions of the membrane monolayers in the region of the diaphragm rim undergo deformations of splay and tilt and accumulate the related elastic energy. These deformations and the corresponding elastic stresses relax along the membranes and become negligibly small at a certain distance from the rim. Hence, the lipid molecules situated at different distances from the diaphragm rim possess different elastic energy. On the other hand, the membrane monolayers must be in lateral equilibrium along their whole area, meaning that the molecular free energy (the chemical potential), μ, of lipids has to be constant along the entire monolayer surfaces, including the regions free from the splay and tilt deformation. This requirement leads to the generation of lateral tensions, γ, in the membrane monolayers to equalize the chemical potential. The relationship between γ and the elastic deformations of splay and tilt is derived in Appendix B.

Numerical calculation of the distribution of the tilt and splay deformations based on Eq. B7 from Appendix B gives the distribution of the lateral tensions over the monolayer surfaces. The result proves to be largely insensitive to the diaphragm radius R and the intermembrane distance H. We illustrate it in Fig. 7 for $R = 2.5$ nm and $H = 6.4$ nm. Fig. 7 *A* represents the distributions of γ in the distal monolayer of an HD, including the diaphragm monolayer ($r < 0$) and that of the expanded stalk ($r > 0$), for two characteristic values of the spontaneous splay, $\tilde{J}_s = -0.11\ \mathrm{nm}^{-1}$ (Fig. 7 *Aa*), corresponding to that of DOPC, and $\tilde{J}_s = -0.34\ \mathrm{nm}^{-1}$ (Fig. 7 *Ab*), describing that of DOPE. Fig. 7 (*Ba* and *Bb*) describes the distribution of the lateral tension in the contacting monolayer for the same parameters as those used in Fig. 7 *A*. Note that the tensions in the monolayers change their signs (Fig. 7 *A* and *B*). This means that there are stretched and compressed monolayer regions, which are, however, in mechanical (and thermodynamical) equilibrium.

The two major features of distribution of the lateral tension are that 1) the tension is concentrated in a rather narrow region around the rim of the diaphragm and 2) within this region in all monolayers γ reaches very high values close to 10 dyn/cm. The maximal tension in the diaphragm monolayers is somewhat smaller than that in the monolayers of the expanded stalk (Fig. 7 *A*). On the other hand, the tension within the diaphragm decays more slowly and hence propagates over a wider region than in the stalk monolayers.

Whereas the total elastic energy of the HD is predicted to be positive for the case of DOPC and negative for DOPE, the distribution of the lateral tensions in the region of the diaphragm rim is similar for the two lipids (Fig. 7 *A* and *B*). In both cases the tension is strongly positive close to the rim in all membrane monolayers, although its maximal value is somewhat smaller for DOPE than for DOPC. The reason for this similarity is that the elastic energy (B3) and hence the lateral tension (B7) are dominated in the rim region by the deformation of tilt, t, which is determined by the packing condition and is independent of the spontaneous splay.

We suggest that the high positive lateral tension, γ, generated along the HD rim results in the rupture of the diaphragm and the formation of the fusion pore. Thus, we predict that the fusion pore is nucleated in some point close to the rim.

Elongated connection

The energy of the elongated connection, F, resulting from linear expansion of the initial stalk is presented in Fig. 8 as a function of the stalk length L for different values of the spontaneous splay, $\tilde{J}_s$. The results are presented for the intermembrane distance $H = 6.4$ nm characterizing the lamellar phases, where formation of these hemifusion intermediates can be expected in the course of transition into *HII* phase. The intercepts of the lines (Fig. 8, *a–d*) give the energies of the initial stalk at the corresponding values of $\tilde{J}_s$. The slopes of the lines (Fig. 8, *a–d*) represent the energy per unit length of the elongated connection. As expected, the more negative the spontaneous splay, $\tilde{J}_s$, the smaller the slope. Spontaneous expansion of the elongated connection becomes energetically favorable for $\tilde{J}_s \approx -0.4\ \mathrm{nm}^{-1}$, which is more negative than the characteristic spontaneous splay of DOPE. Hence, according to our model, the evolution of the initial hemifusion intermediate into an elongated connection is unlikely to be possible. This conclusion is supported by comparison of the energy of the elongated connection with that of the HD. Fig. 9 presents the energy per unit length of the elongated connection (Fig. 9 *a*) and the energies per unit length of circumference of the diaphragm rim for the same intermembrane distance $H = 6.4$ nm and for different values of the HD radius (Fig. 9, *b–d*). Clearly, the HD energy is considerably smaller than that of the elongated connection for all realistic values of the spontaneous splay, $\tilde{J}_s$. The reason for the difference in the energy of the two types of fusion intermediates is, clearly, related to their structures. The elongated connection represents a junction of four membranes, whereas the HD rim is a three-junction of bilayers. The tilt angle, ϕ, in each monolayer in a four-junction is $\pi/4$, whereas in the three-junction the tilt angles α, β, and γ (Appendix C) are close to $\phi = \pi/6$. The smaller tilt results in lower energy.

We predict that evolution of the initial stalk proceeds via its expansion into an HD rather than an elongated connection.

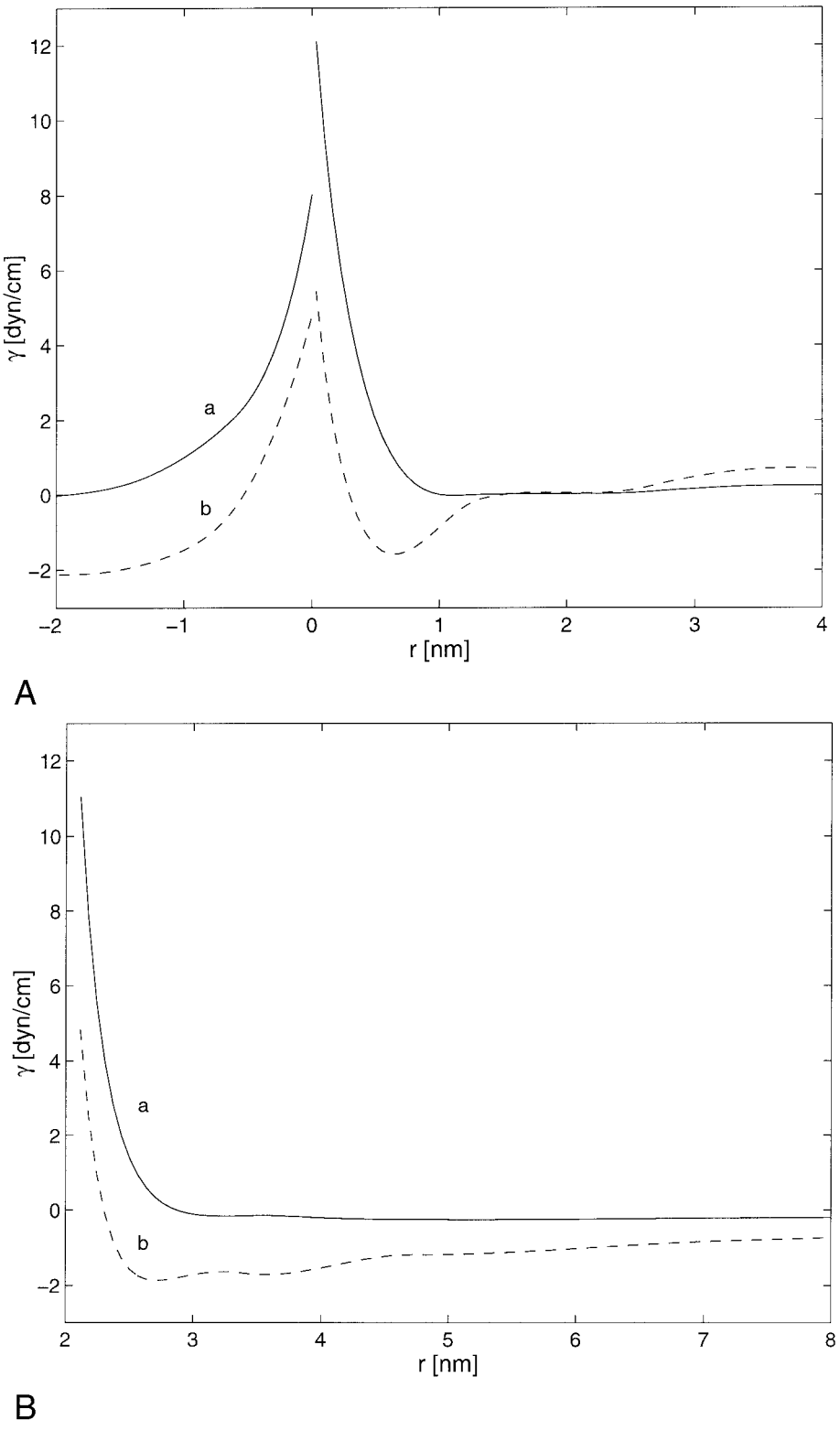

FIGURE 7 Distribution of lateral tension along the monolayers of the hemifusion diaphragm with the intermembrane distance $H = 6.4$ nm and the diaphragm radius $R = 4$ nm. (*A*) Distal monolayer; $r < 0$ corresponds to the flat diaphragm and $r > 0$ corresponds to the expanded stalk: (*a*) $\tilde{J}_s = -0.11$ nm^{-1}; (*b*) $\tilde{J}_s = -0.34$ nm^{-1}. (*B*) Contacting monolayer: (*a*) $\tilde{J}_s = -0.11$ nm^{-1}; (*b*) $\tilde{J}_s = -0.34$ nm^{-1}.

DISCUSSION

The pathway of evolution of the initial intermediate of membrane fusion, the fusion stalk, toward the final intermediate, the expanding fusion pore, poses a challenge to both experimental and theoretical studies. In particular, whereas the known effects of the lipid composition of the distal membrane monolayers on fusion suggest that the initial fusion pore forms in the

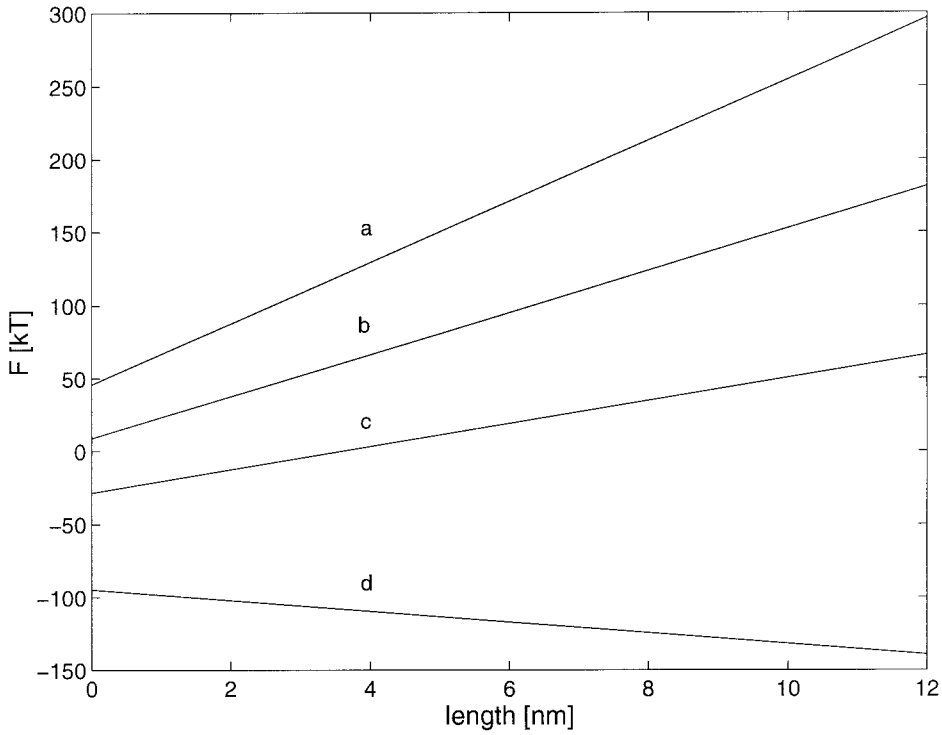

FIGURE 8 Energy of the elongated connection as a function of its length for different values of the spontaneous splay: (*a*) $\tilde{J}_s = -0.11\ \mathrm{nm}^{-1}$; (*b*) $\tilde{J}_s = -0.22\ \mathrm{nm}^{-1}$; (*c*) $\tilde{J}_s = -0.34\ \mathrm{nm}^{-1}$; (*d*) $\tilde{J}_s = -0.55\ \mathrm{nm}^{-1}$.

HD, recent theoretical work has argued against stalk expansion into the HD. Thus, the specific question is whether the fusion stalk expands and gives rise to an HD or, alternatively, transforms directly into a fusion pore via local rearrangements of the membrane structure. We address this problem theoretically, using a recently developed elastic model (Hamm and Kozlov, 1998, 2000; Kozlovsky and Kozlov, 2002; May, 2000).

Conditions for HD formation: strongly negative spontaneous splay or pulling force

We found that out of two possible hemifusion intermediates, which may be produced by the stalk expansion, a circular HD, and an elongated intermembrane connection, the former is always more favorable energetically than the

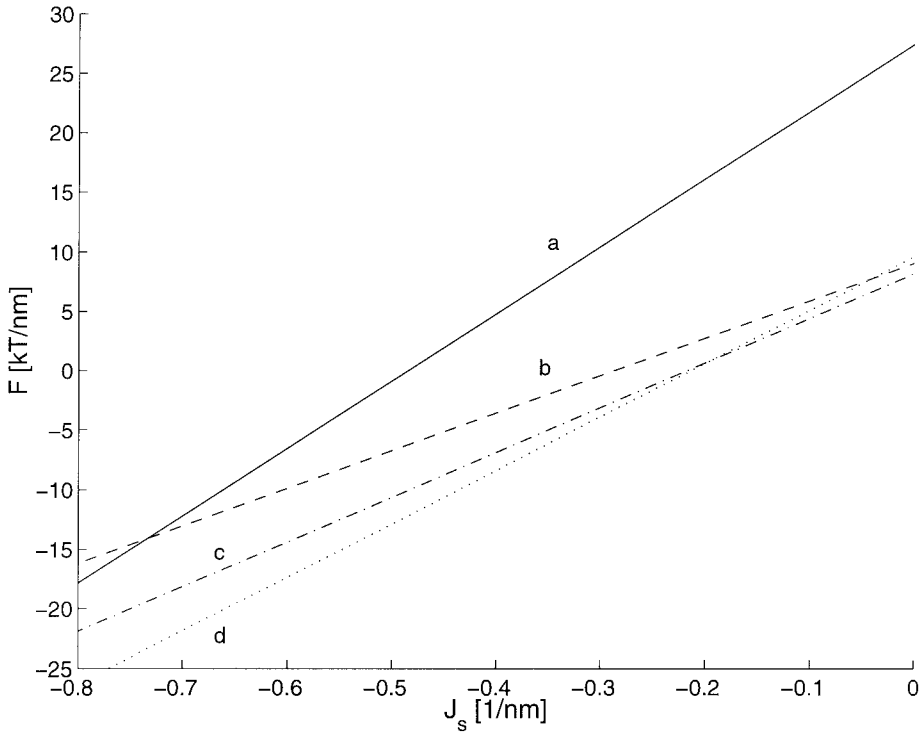

FIGURE 9 Comparison of the energy per unit length of the circumference of the hemifusion diaphragm with that of the elongated connection. The energy is represented as a function of the spontaneous splay for different values of the diaphragm radius, *R*: (*a*) elongated connection; (*b*) $R = 1.2$ nm; (*c*) $R = 2.5$ nm; (*d*) $R = 25$ nm.

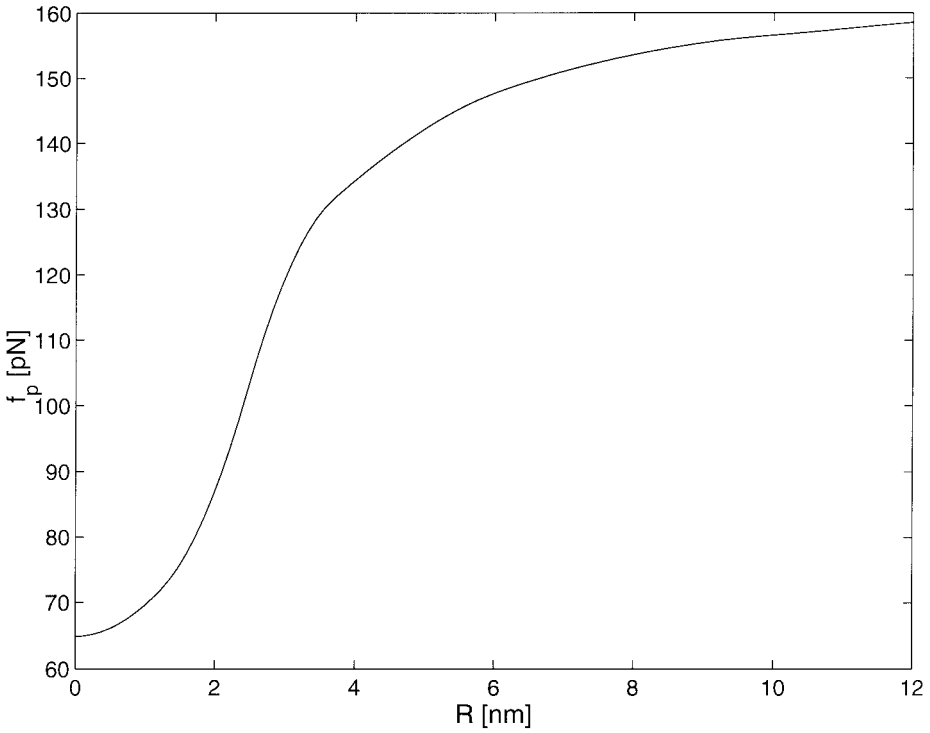

FIGURE 10 Dependence of the equilibrium diaphragm radius on the force pulling the rim of the hemifusion diaphragm apart. The spontaneous splay is $\tilde{J}_s = -0.11$ nm^{-1}, the intermembrane distance is $H = 13$ nm, and the width of the expanded stalk is $r = 25$ nm.

latter. The intrinsic tendency of a fusion stalk to expand into an HD is controlled by the spontaneous splay, $\tilde{J}_s$, of the contacting monolayers of the fusing membranes.

For positive or moderately negative values of $\tilde{J}_s$, expansion of the fusion stalk is energetically unfavorable ((Fig. 4 *a*) dotted and dashed curves), meaning that, if the stalk forms because of thermal fluctuations, it will not transform *spontaneously* into an HD. However, even in these conditions an HD can form, provided that an external force pulling apart the diaphragm rim is developed in the system. In the case of biological fusion, such a force can come from the specialized membrane proteins referred to as fusion proteins (Jahn and Sudhof, 1999; Kozlov and Chernomordik, 2002; Skehel and Wiley, 2000). The results of the present model allow estimation of the value of the pulling force necessary to expand the fusion stalk into an HD for different lipid compositions. The pulling force, f_p, which equilibrates the intrinsic resistance of the diaphragm to expansion, is related to the HD elastic energy, $F(R)$, by $f_p = dF/dR$. The derivative dF/dR, represented graphically by the slope of the function $F(R)$, increases with the diaphragm radius R (Fig. 4 *a*). Therefore, to achieve a larger value of the diaphragm radius R, a stronger force f_p has to be applied to the HD rim. This is illustrated in Fig. 10 for membranes consisting of a common lipid, DOPC, with the spontaneous splay $\tilde{J}_s^{DOPC} \approx -0.11$ nm^{-1} and for the intermembrane distance $H = 13$ nm, established in the presence of fusion proteins such as influenza HA trimer. The minimal pulling force, f_p, necessary to start expansion of an HD constitutes $f_p \approx 65$ pN, whereas formation of an HD of ~20 nm in diameter requires a force of $f_p \approx 150$ pN. Mixing DOPC with such lipids as DOPE, which has $\tilde{J}_s^{DOPE} \approx -0.35$ nm^{-1}, results in a more negative $\tilde{J}_s$ of the monolayer and hence decreases the required pulling force.

How many fusion proteins are needed to generate this kind of force? Assuming that one HA generates ~10 pN of pulling force (estimate from (Kozlov and Chernomordik 1998)), multiple (for instance, 6 or 7) trimers are needed to initiate stalk expansion for DOPC bilayers. Even more proteins are necessary to further expand the fusion diaphragm (Fig. 10). An example of a specific mechanism for generation of a large pulling force by concerted action of multiple fusion proteins is suggested by the fusion coat hypothesis (Kozlov and Chernomordik, 2002).

The considerations above can be applied to the analysis of the experimental results on HD formation. The spontaneous splay of monolayers of cell membranes is unknown, as their compositions are highly variable and may change along the membrane plane. However, a reasonable suggestion is that the average $\tilde{J}_s$ of cell monolayers is close to that of DOPC or slightly more negative, because of the presence of lipids like DOPE. Therefore, a fairly large number of fusion proteins is needed for HD expansion to dimensions that are detectable by electron microscopy. The fact that no HD has been observed in cell systems (Frolov et al., 2000) can indicate that the monolayer spontaneous splay in the fusion sites was not sufficiently negative and probably was close to that of DOPC. Note, however, that detection of the extended HD can be hindered not only when the pulling force is insufficient but also when the HD rapidly transforms into fusion pores. More quantitative

analysis requires specific measurements of $\tilde{J}_s$ in the fusion site and of the number of fusion proteins associated with one fusion intermediate.

Implications for lamellar-inverted hexagonal phase transition in lipid systems

We predict that the stalk will expand spontaneously into an HD with limited radius provided that the spontaneous splay of the monolayers, $\tilde{J}_s$, enters the range between the two negative characteristic values, $\tilde{J}_s^{**} < \tilde{J}_s < \tilde{J}_s^{*}$, which depend on the constraints. If $\tilde{J}_s$ becomes even more negative, $\tilde{J}_s \leq \tilde{J}_s^{**}$, the HD grows infinitely. Spontaneous formation of HD with infinite edge means that the membrane system tends to transform into a straight three-junction of bilayers. A lipid phase consisting of straight three-junctions is the inverted hexagonal (*HII*) phase. Therefore, the results we have obtained for the case of $H = 6.4$ nm, which corresponds to the intermembrane distance in the lamellar (L) phases (Rand and Parsegian, 1989) can help to understand the L-to-*HII* phase transition of lipids.

It has been demonstrated (Gawrisch et al., 1992), in agreement with (Kozlov et al., 1994; Laradji et al., 1997; Li and Schick, 2000) and the present model, that gradual change of the spontaneous splay (spontaneous curvature), $\tilde{J}_s$, of DOPE membranes towards negative values results in the L-to-*HII* transition at a specific value of $\tilde{J}_s$. Are there any intermediate structures between the L and *HII* phases? Based on our results for $H = 6.4$ nm (Fig. 5 *c*) a phase of HDs with limited radius R^* is expected to form within a broad range of the spontaneous splay, $-0.32\ \mathrm{nm}^{-1} < \tilde{J}_s < -0.21\ \mathrm{nm}^{-1}$. However, no intermediate phases were detected in the experimental studies (Siegel et al., 1989, 1994; Siegel and Epand, 1997). To reconcile our theoretical prediction with these experimental data we suggest the following explanation.

On the way to HD formation, the membranes have to overcome an energy barrier, F_B, represented by the energy of the initial stalk and, most probably, an additional energy related to rupture of the apposing lipid monolayers necessary for stalk formation (Leikin et al., 1987). This barrier has to become sufficiently small to allow for membrane fusion within the experimental time scale. Our computations show that the contribution to F_B from the initial stalk vanishes for $H = 6.4$ nm at $\tilde{J}_s^f \approx -0.25\ \mathrm{nm}^{-1}$. In case the related decrease of F_B is sufficient for fusion to occur, multiple isolated HDs of radius $R^* \approx 2$ nm would form (Fig. 5 *c*). According to the suggestion of Siegel (1999), a membrane-mediated attractive interaction develops between the isolated HDs resulting in their mutual approach and clusterization. This reduces, effectively, the areas of the constrained wings of HDs and, thus, decrease the overall energy (Siegel, 1999). The clusterized HDs become, effectively, unconstrained, and their radii described by the curve (Fig. 5 *a*) increase up to $R^* \approx 3$ nm, as illustrated by (Fig. 5 *d*). This scenario still does not solve the problem. However, provided that the needed reduction of the barrier F_B requires a little more negative spontaneous splay, such as $\tilde{J}_s^f \leq -0.27\ \mathrm{nm}^{-1}$, the initially formed HDs of $R^* \approx 2.3$ nm tend, as a result of their interaction and clusterization, to extend their rims infinitely (Fig. 5 *e*), thus, giving rise to *HII* phase formation.

The approximate character of our model does not allow to compute the spontaneous splay of fusion, $\tilde{J}_s^f$, with accuracy accounting for the subtle difference between the values above. For example, we neglect the small effects of the saddle-splay deformations (Hamm and Kozlov, 1998, 2000) on the stalk energy (Kozlovsky and Kozlov, 2002). Accounting for these effects based on the value for the monolayer modulus of Gaussian curvature calculated in Szleifer et al., (1990) results in a shift of $\tilde{J}_s^f$ to a value of $\approx -0.28\ \mathrm{nm}^{-1}$, and, thus, predicts the unlimited expansion of HD. It is also uncertain whether the experimental methods used were sufficiently sensitive to account for such small changes in the spontaneous splay of the monolayers, $\tilde{J}_s^f$. Therefore, we conclude, in agreement with the experimental data, that in major cases, the ultimate product of membrane fusion in the L phases should be the straight three-junctions forming the *HII* phase.

Mechanism of fusion pore formation

In the stalk-pore hypothesis, formation of a fusion pore is promoted by the lateral tension, γ, developed in the diaphragm. This is analogous to pore formation in a number of phenomena such as lysis and electroporation of cells, liposomes, and planar bilayers (Abidor et al., 1979; Brochard-Wyart et al., 2000; Lieber and Steck, 1989; Needham and Hochmuth, 1989; Weaver and Chizmadzhev, 1996). In artificial systems such as two fusing planar bilayers (for review, see Chernomordik et al., 1987) or osmotically driven fusion of liposomes with a planar bilayer (Chanturiya et al., 1997; Chernomordik et al., 1995a; Zimmerberg et al., 1980), the physical reasons for the tension in an HD are obvious. However in the case of two cell membranes fusing because of the action of specialized membrane proteins, the factors, which can produce tension, are largely unknown. A qualitative mechanism for tension generation directly by the fusion proteins has been proposed recently (Kozlov and Chernomordik, 2002). In the present work, we suggest an additional source for tension in HDs, originating from the elastic stresses of tilt and splay in the region of the diaphragm rim. This tension is developed as a result of establishment of lateral equilibrium between the lipid molecules situated in the deformed monolayer regions close to the rim and those forming the stress-free regions of the membranes. We show that the resulting lateral tension reaches very high values of $\sim\gamma_m \approx 10$ dyn/cm in each monolayer, yielding a bilayer tension close to $\gamma_B \approx 20$ dyn/cm. However, this

tension rapidly decays with distance from the diaphragm rim.

A characteristic time of pore formation depends on both the lateral tension and the area of the stressed membrane. The larger the area, the higher the probability of pore formation within a given time span and under a given tension (Chernomordik et al., 1987). The usual tension resulting within a realistic time span in pore formation in the membranes of small unilamellar vesicles (SUV) with a diameter of ~40 nm is $\gamma_B \approx 10$ dyn/cm (Brochard-Wyart et al., 2000; Taupin, 1975). Although the stressed area around the HD rim is smaller than that of an SUV, the tension, γ_B, is twice as large and hence may be sufficient to rupture the membrane. Whereas additional factors may be involved in HD destabilization, the localized tension makes the rim of the HD the most probable place for the opening of a fusion pore. Expansion of the diaphragm accompanied by an increase in the HD perimeter, and hence in the growth of the stressed area, accelerates membrane rupture.

An interesting prediction following from our model is that a fusion pore is expected to expand along the diaphragm rim and thus to adopt an elongated shape. This is different from the usual circular pores formed in homogeneously stressed membranes.

Note that, according to our results, the tension is generated, and, thus the pores can form, both within the diaphragm itself and in the portions of the membranes of the expanded stalk bounding the diaphragm. A more detailed analysis is needed to predict which of the two events is more probable.

Assumptions of the model

Our analysis is based on a continuous elastic description of the structure and energy of the HD rim implying several basic assumptions, which have to be discussed.

We assume the membranes to be homogeneous at least within the region where the fusion intermediate is formed. Therefore, the elastic constants such as the bending modulus, κ, the tilt modulus, κ_t, and the spontaneous splay, $\tilde{J}_s$, do not change along the membrane surface. According to the experimental and theoretical studies of lipid bilayers consisting of mixtures of DOPC, DOPE, LPC, and other phospholipids, this assumption describes well the elastic properties of synthetic membranes (see, e.g., Chen and Rand, 1997; Fuller and Rand, 2001; Gawrisch et al., 1992; Leikin et al., 1996). However, compositions of the fusion sites of biological membranes may be inhomogeneous, contain cholesterol-enriched domains (referred to as membrane rafts), and inserted proteins (Lang et al., 2001). Therefore, the predictions of the present model if applied to biological fusion should be considered on a qualitative rather than quantitative level.

For our analysis we use a continuum description of a lipid monolayer based on a elastic model quadratic in deformations (Frank, 1958; Hamm and Kozlov, 2000; Helfrich, 1973). This approach requires that the length scale of the monolayer deformations is considerably larger than the cross-section of a hydrophobic chain of a lipid molecule and that the deformations remain small. As discussed in detail in Kozlovsky and Kozlov (2002), whereas the two sets of conditions are satisfied along the major part of the membrane, they are nearly violated in a narrow region around the HD rim, where the splay deformation changes considerably over just several (seven to eight) hydrocarbon chains and the tilt deformation approaches the value of one. This gives another reason for considering the predictions of the present model as qualitative rather than quantitative ones. However, application of this model is justified by the previous analysis of the elastic properties of *HII* phases (Hamm and Kozlov, 1998; Kozlov et al., 1994; Kozlov and Winterhalter, 1991; Leikin et al., 1996) where, similarly to the HD rim, the splay deformations change within a molecular scale, and the deformations reach large values. Quantitative agreement between the theory and the experiment for the *HII* phases strongly supports application of our approach for analysis of the fusion intermediates.

Another assumption consists in neglecting the effects of the saddle-splay deformations, which include the Gaussian curvature of monolayers and the variation of the tilt of the hydrocarbon chains along the monolayer surface (Frank, 1958; Hamm and Kozlov, 2000; Helfrich, 1973). Based on the Gauss-Bonnet theorem, the energy of the Gaussian curvature depends only on the topology (genus) of the monolayers (Helfrich, 1973). In the simplified model, which does not account for the monolayer tilt (Fig. 11 *a*), the membrane topology does not change in the course of stalk evolution into an HD or an elongated connection. As a result, the Gaussian curvature gives a constant energy contribution to all fusion intermediates, and, therefore, does not influence the conclusions of the analysis. In the more sophisticated model considered in this study, on one hand, the energy of the changing tilt does not strictly fulfill the Gauss-Bonnet theorem (Hamm and Kozlov, 2000), and on the other the surface integral of the Gaussian curvature is not strictly constant because of the dependence of the HD angle, φ (Fig. 1 *c*), on the HD radius, *R*. However, according to our estimations, these two effects largely compensate for each other, and the corrections to the energy of HD and the elongated connection are negligibly small. Discussion of the saddle-splay energy in the context of formation of the initial fusion stalk is presented in Kozlovsky and Kozlov (2002).

Comparison with previous models

In contrast to previous studies, the present model predicts formation of an HD to be favored in a feasible range of $\tilde{J}_s$, a range that characterizes membranes consisting of DOPE and its mixtures with other lipids. The possible formation of infinitely large HDs has also been discussed in Markin and

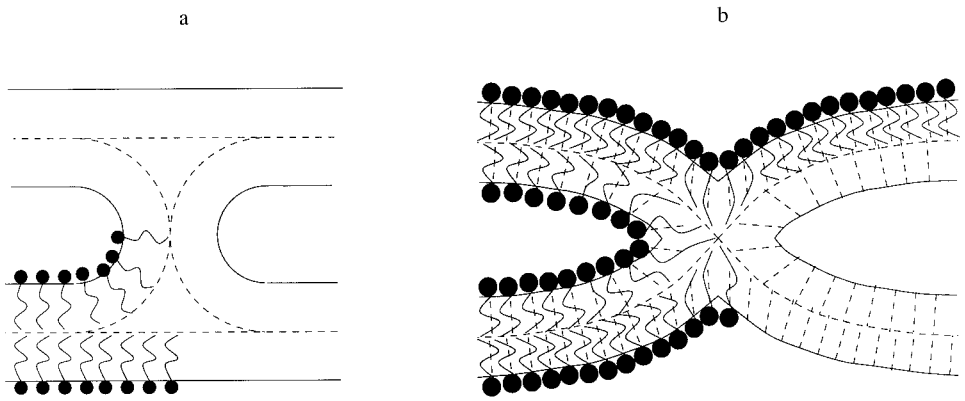

FIGURE 11 Structure of a fusion stalk. (*a*) First model with empty interstices. (*b*) Current model with interstices filled by tilting the hydrocarbon chains.

Albanesi (2002). This difference in results originates from the assumptions about the structure of the diaphragm rim discussed in detail elsewhere (Kozlovsky and Kozlov, 2002) in the context of the study of stalk structure.

The major factor making the diaphragm energetically unfavorable in the previous model (Siegel, 1993, 1999) is the hydrophobic interstice generated along the diaphragm rim because of chain packing in the region of merger of two bilayers into one. The interstice has been modeled as an empty void requiring a large energy price for its formation. It has been mentioned in the literature that heterogeneity of the lipids in biological membranes and, in particular, the presence of apolar lipids can dramatically decrease the energy price of these voids (Chernomordik et al., 1995b; Walter et al., 1994). In this work, we do not rely on any membrane impurities. We suggest that the hydrocarbon chains of the lipid molecules fill the voids so that no vacuum is left in the system. This is achieved by tilting the hydrocarbon chains with respect to the membrane surface so that the energy of the empty voids is replaced by the energy of the tilt deformation. In addition, we allow the monolayer profiles to form sharp corners along the lines facing the interstices. Counterintuitively, this feature of the membrane shape does not result in infinite elastic energy (Kozlovsky and Kozlov, 2002) but rather reduces, effectively, the total area of deformed monolayers. The resulting overall energy of the monolayer deformation is few times smaller than that obtained previously. Because the system tends to adopt a configuration of minimal energy, the structure of the HD and the predictions about its evolution following from our model have to be closer to reality than those suggested previously.

CONCLUSIONS

We show that a fusion stalk spontaneously expands into an HD provided that the contacting monolayers of the fusing membranes consist of lipids with sufficiently negative spontaneous splay, $\tilde{J}_s$, such as DOPE or its mixtures with other lipids.

In case the spontaneous splay is close to that of a common lipid, DOPC, the HD can be formed when an external force, generated by the fusion proteins, pulls apart the diaphragm rim.

We show that the elastic stresses of tilt and splay of the hydrocarbon chains developed in the region of the diaphragm rim generate the lateral tension. This tension can be sufficiently large to result in formation of a fusion pore expanding along the rim and leading to completion of the fusion reaction. In contrast to recent models suggesting direct transition from a stalk to a pore, the results of our analysis indicate the possibility of HD expansion followed by fusion pore formation. This explains the known effects of the lipid composition of the inner membrane monolayers on fusion pores.

APPENDIX A

Structure of the fusion stalk

Formation of a stalk can be presented as a two-step process. First, the contacting monolayers of the two membranes undergo strong bending and form an intramembrane connection, illustrated in Fig. 11 *a*, which represents the first model of a fusion stalk (Chernomordik et al., 1995b; Kozlov and Markin, 1983; Markin et al., 1984). A void, referred to as a hydrophobic interstice, is formed inside this structure in the region between the apposing differently curved portions of the monolayers (Fig. 11 *a*). Filling this void by hydrocarbon chains requires a second step of deformation, which consists in the tilt of the hydrocarbon chains facing the interstice with respect to the monolayer surface (Fig. 11 *b*). This tilt model of the hydrophobic interstice, first suggested in the context of the inverted hexagonal (*HII*) phases of phospholipids (Hamm and Kozlov, 1998, 2000) constitutes the essence of the new approach to the analysis of the stalk intermediate. The chain tilt decays from the center towards the periphery of the stalk and gives rise to splay of the hydrocarbon chains, which interferes with the splay induced initially by the bending of the monolayer (Hamm and Kozlov, 1998, 2000). As a result of the combined deformations of bending and tilt, the profiles of the monolayers form sharp corners in front of the stalk center (Fig. 11). While unusual in the context of the earlier

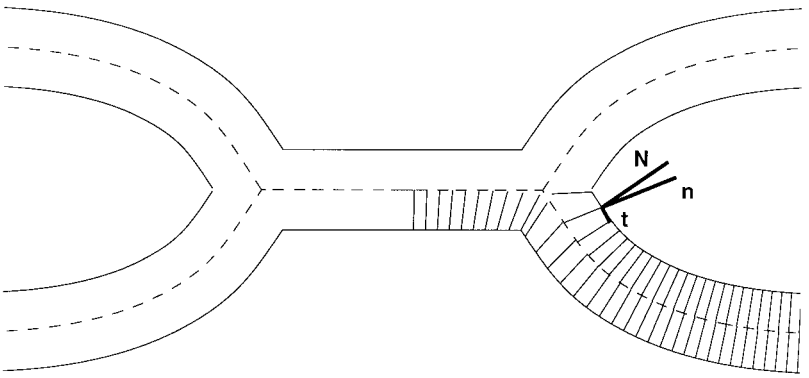

FIGURE 12 Structure of hemifusion diaphragm: notations.

models, this stalk structure proved to be self-consistent, exhibiting moderate local deformations of splay and tilt of the hydrocarbon chains and possessing energy much lower than that predicted previously, thus, solving the "energy crisis" of the stalk model (Kozlovsky and Kozlov, 2002).

APPENDIX B

Elastic model

The details of the elastic model for the deformations of splay and tilt are presented elsewhere (Kozlovsky and Kozlov, 2002). Here we sketch its major points.

Monolayer deformations

The conformation of a monolayer is characterized by its shape and the average orientation of the hydrocarbon chains of the lipid molecules with respect to the membrane surface.

We identify the monolayer shape with that of the dividing surface (Fig. 12), which lies along the interface between the polar heads and the hydrocarbon tails of lipid molecules and has been shown for some lipids to play a role of the neutral surface (Kozlov et al., 1994; Leikin et al., 1996). The shape of the monolayer is determined by the orientation of the normal vector $\vec{N}$ at each point of the dividing surface.

To characterize the average orientation of hydrocarbon chains, we use a unit vector, $\vec{n}$, referred to as the chain director (Fig. 12). The chain director, $\vec{n}$, can vary along the dividing surface, describing a changing orientation of the chains.

The major contributions to the elastic energy of the monolayer come from the tilt, $\vec{t}$, of the hydrocarbon chains with respect to the membrane surface and from the splay, $\tilde{J}$, of the chains. Mathematically, tilt is described by deviation of the chain director, $\vec{n}$, from the surface normal, $\vec{N}$, according to

$$\vec{t} = \frac{\vec{n}}{\vec{n} \cdot \vec{N}} - \vec{N} \qquad \text{(B1)}$$

The splay can be expressed as a covariant divergence of the chain director along the dividing surface,

$$\tilde{J} = \operatorname{div} \vec{n} \qquad \text{(B2)}$$

There are two factors that contribute to the splay of the chains (Hamm and Kozlov, 1998, 2000). The first is the total curvature, J, of the dividing surface (Helfrich, 1973), and the second is the variation of the tilt, $\vec{t}$, along the dividing surface (Frank, 1958).

Elastic energy of the monolayer

The elastic properties of a lipid monolayer are characterized by the spontaneous values of its splay and tilt and by the elastic moduli related to the splay and tilt deformations.

The spontaneous splay, $\tilde{J}_s$, is directly manifested in the shapes of lipid monolayers formed as a result of self-assembly of phospholipids in aqueous solutions (Luzzati, 1968). Its values for typical classes of phospholipids such as LPC, DOPC, and DOPE are presented in the main part of the paper. The spontaneous splay of a mixed monolayer is well described by a weighted average of the spontaneous splays of its components (Kozlov and Helfrich, 1992).

In the direction along the membrane plane, a monolayer in the liquid crystalline state has the properties of an isotropic two-dimensional fluid and therefore has no spontaneous tilt.

The splay elastic modulus, κ, has been measured for the deformation of pure bending (Niggemann et al., 1995) and referred to as the bending modulus (Helfrich, 1973). Its value for lipid monolayers is $\kappa \approx 4 \times 10^{-20}$ J. The tilt elastic modulus, κ_t, has not been measured directly. Its value, based on fitting of indirect experimental data (Hamm and Kozlov, 1998) supported by theoretical estimation (Hamm and Kozlov, 2000; May and Ben-Shaul, 1999) can be estimated as $\kappa_t \approx 40$ mN/m.

The elastic energy, f, of splay and tilt per unit area of the dividing surface related to the energy of a flat monolayer, $J = 0$, with vanishing tilt, $\vec{t} = 0$, is given for the case of small deformations by

$$f = \tfrac{1}{2} \cdot \kappa \cdot (\operatorname{div} \vec{n} - \tilde{J}_s)^2 + \tfrac{1}{2} \cdot \kappa_t \cdot t^2 - \tfrac{1}{2} \cdot \kappa \cdot \tilde{J}_s^2, \qquad \text{(B3)}$$

The total elastic energy, F, is determined by integration of Eq. (B3) over the dividing surfaces of all monolayers constituting the hemifusion intermediate

$$F = \int f dA. \qquad \text{(B4)}$$

Lateral tension induced by elastic deformations

The distribution of the lateral tension, γ, over the area of a monolayer can be found using the Gibbs relationship between the surface tension and the chemical potential, $d\mu = -a \cdot d\gamma$, in which a is the area per molecule in the membrane plane. Integration of this equation, assuming that the monolayer is practically incompressible so that the molecular area, a, does not depend on the tension, γ, gives

$$\mu = \mu_0 - a \cdot \gamma. \qquad \text{(B5)}$$

The first contribution, μ_0, corresponding to the chemical potential at a vanishing tension, can be presented as a sum of the elastic energy per

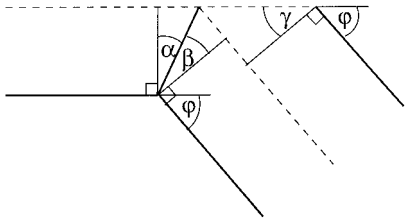

FIGURE 13 Boundary conditions on the rim of a hemifusion diaphragm.

molecule, μ_{el}, and the chemical potential, μ^0, in the stress-free state, so that the chemical potential is

$$\mu = \mu^0 + \mu_{el} - a \cdot \gamma. \quad \text{(B6)}$$

According to the condition of lateral equilibrium, μ is constant over the whole monolayer surface including the completely stress-free area far from the diaphragm rim, meaning that $\mu = \mu^0$. The resulting equation for the lateral equilibrium is $\mu_{el} = a \cdot \gamma$. The elastic contribution to the chemical potential is $\mu_{el} = a \cdot f$, where the energy per unit area, f, is given by Eq. B3. As a result, the lateral tension in a monolayer is

$$\gamma = \tfrac{1}{2} \cdot \kappa \cdot (\mathrm{div}\, \vec{n} - \tilde{J}_s)^2 + \tfrac{1}{2} \cdot \kappa_t \cdot t^2 - \tfrac{1}{2} \cdot \kappa \cdot \tilde{J}_s^2 \quad \text{(B7)}$$

APPENDIX C

Boundary conditions at the HD rim

The HD rim is formed by the joining of three bilayers: the two bilayers of the expanded stalk and the bilayer of the diaphragm. Because the structure is symmetrical we consider its representative element (Fig. 13), which consists of the contacting and distal monolayers of the expanded stalk and the HD monolayer joint to the distal monolayer. The membrane configuration is characterized by four angles (Fig. 13): the angle φ between the midsurface of the expanded stalk and the surface of the HD, and the three tilt angles at the rim, α, β, γ, which characterize the diaphragm, distal, and contacting monolayers, respectively.

We assume that the monolayers are incompressible and have constant surface area per lipid molecule. The homogeneous tilt of the chains does not affect the monolayer thickness, d, but is accompanied by chain stretching (Hamm and Kozlov, 2000; Kozlovsky and Kozlov, 2002). Therefore, we assume d to be constant all over the system. Note that this assumption neglects the effect of splay on d (Hamm and Kozlov, 2000). However, the related corrections to the elastic energy (Eq. B3) are of a higher order than those taken into account by our model. According to our numerical estimations, these corrections are indeed negligibly small.

The assumptions above result in the following relationships representing the boundary conditions for the membrane configurations: the characteristic angles have to satisfy $\alpha = \beta = \varphi/2$ and $\gamma = \pi/2 - \varphi$, and the chain length in the junction point has to be equal to $d/\cos\alpha$.

We are grateful to Fredric Cohen, Kirill Katsov, Barry Lentz, Gregory Melikyan, Michael Schick, David Siegel, and Joshua Zimmerberg for enjoyable discussions. M.K. is grateful to the Israel Science Foundation and the Human Frontier Science Program Organization for the financial support.

REFERENCES

Abidor, I. G., V. B. Arakelyan, L. V. Chernomordik, Y. A. Chizmadzhev, V. F. Pastushenko, and M. R. Tarasevich. 1979. Electrical breakdown of BLM: main experimental facts and their qualitative discussion. *Bioelectrochem. Bioenerg.* 6:37–52.

Brochard-Wyart, F, P. G. de Gennes, and O. Sandre. 2000. Transient pores in stretched vesicles: role of leak-out. *Physica A.* 278:32–51.

Chandler, D. E., and J. E. Heuser. 1980. Arrest of membrane fusion events in mast cells by quick-freezing. *J. Cell Biol.* 86:666–674.

Chanturiya, A., L. V. Chernomordik, and J. Zimmerberg. 1997. Flickering fusion pores comparable with initial exocytotic pores occur in protein-free phospholipid bilayers. *Proc. Natl. Acad. Sci. U.S.A.* 94: 14423–14428.

Chen, Z., and R. P. Rand. 1997. The influence of cholesterol on phospholipid membrane curvature and bending elasticity. *Biophys. J.* 73: 267–276.

Chernomordik, L., A. Chanturiya, J. Green, and J. Zimmerberg. 1995a. The hemifusion intermediate and its conversion to complete fusion: regulation by membrane composition. *Biophys. J.* 69:922–929.

Chernomordik, L., M. Kozlov, and J. Zimmerberg. 1995b. Lipids in biological membrane fusion. *J. Membr. Biol.* 146:1–14.

Chernomordik, L. V., V. A. Frolov, E. Leikina, P. Bronk, and J. Zimmerberg. 1998. The pathway of membrane fusion catalyzed by influenza hemagglutinin: restriction of lipids, hemifusion, and lipidic fusion pore formation. *J. Cell. Biol.* 140:1369–1382.

Chernomordik, L. V., E. Leikina, V. Frolov, P. Bronk, and J. Zimmerberg. 1997. An early stage of membrane fusion mediated by the low pH conformation of influenza hemagglutinin depends upon membrane lipids. *J. Cell Biol.* 136:81–94.

Chernomordik, L. V., G. B. Melikyan, I. G. Abidor, V. S. Markin, and Y. A. Chizmadzhev. 1985. The shape of lipid molecules and monolayer membrane fusion. *Biochim. Biophys. Acta.* 812:643–655.

Chernomordik, L. V., G. B. Melikyan, and Y. A. Chizmadzhev. 1987. Biomembrane fusion: a new concept derived from model studies using two interacting planar lipid bilayers. *Biochim. Biophys. Acta.* 906(3): 309–352.

Ellens, H., J. Bentz, and F. C. Szoka. 1985. H+- and Ca2+-induced fusion and destabilization of liposomes. *Biochemistry.* 24:3099–3106.

Frank, F. C. 1958. On the theory of liquid crystals. *Discuss. Faraday. Soc.* 25:19–28.

Frolov, V., M.-S. Cho, P. Bronk, T. Reese, and J. Zimmerberg. 2000. Multiple local contact sites are induced by GPI-linked influenza hemagglutinin during hemifusion and flickering pore formation. *Traffic.* 1:622–630.

Fuller, N. L., and R. P. Rand. 2001. The influence of lysolipids on the spontaneous curvature and bending elasticity of phospholipid membranes. *Biophys. J.* 81:243–254.

Gaudin, Y., C. Tuffereau, P. Durrer, J. Brunner, A. Flamand, and R. Ruigrok. 1999. Rabies virus-induced membrane fusion. *Mol. Membr. Biol.* 16:21–31.

Gawrisch, K., V. A. Parsegian, D. A. Hajduk, M. W. Tate, S. M. Graner, N. L. Fuller, and R. P. Rand. 1992. Energetics of a hexagonal-lamellar-hexagonal-phase transition sequence in dioleoylphosphatidylethanolamine membranes. *Biochemistry.* 31:2856–2864.

Gingell, D., and I. Ginsberg. 1978. Problems in the physical interpretation of membrane interaction and fusion. *In* Membrane Fusion. G. Poste and G. L. Nicholson, editors. Elsevier, Amsterdam. 791–833.

Grote, E., M. Baba, Y. Ohsumi, and P. J. Novick. 2000. Geranylgeranylated SNAREs are dominant inhibitors of membrane fusion. *J. Cell Biol.* 151:453–466.

Hamm, M., and M. Kozlov. 1998. Tilt model of inverted amphiphilic mesophases. *Eur. Phys. J. B.* 6:519–528.

Hamm, M., and M. Kozlov. 2000. Elastic energy of tilt and bending of fluid membranes. *Eur. Phys. J. E.* 3:323–335.

Helfrich, W. 1973. Elastic properties of lipid bilayers: theory and possible experiments. *Z. Naturforsch.* 28c:693–703.

Helm, C. A., J. N. Israelachvili, and P. M. McGuiggan. 1989. Molecular mechanisms and forces involved in the adhesion and fusion of amphiphilic bilayers. *Science.* 246:919–922.

Hui, S. W., T. P. Stewart, L. T. Boni, and P. L. Yeagle. 1981. Membrane fusion through point defects in bilayers. *Science.* 212:921–923.

Jahn, R., and T. C. Sudhof. 1999. Membrane fusion and exocytosis. *Annu. Rev. Biochem.* 68:863–911.

Kemble, G. W., T. Danieli, and J. M. White. 1994. Lipid-anchored influenza hemagglutinin promotes hemifusion, not complete fusion. *Cell.* 76:383–391.

Kozlov, M. M., and L. V. Chernomordik. 1998. A mechanism of protein-mediated fusion: coupling between refolding of the influenza hemagglutinin and lipid rearrangements. *Biophys. J.* 75:1384–1396.

Kozlov, M. M., and L. V. Chernomordik. 2002. The protein coat in membrane fusion: lessons from fission. *Traffic.* 3:256–267.

Kozlov, M. M., and W. Helfrich. 1992. Effects of a cosurfactant on the stretching and bending elasticities of a surfactant monolayer. *Langmuir.* 8:2792–2797.

Kozlov, M. M., S. Leikin, and R. P. Rand. 1994. Bending, hydration and void energies quantitatively account for the hexagonal-lamellar-hexagonal reentrant phase transition in dioleoylphosphatidylethanolamine. *Biophys. J.* 67:1603–1611.

Kozlov, M. M., S. L. Leikin, L. V. Chernomordik, V. S. Markin, and Y. A. Chizmadzhev. 1989. Stalk mechanism of vesicle fusion: intermixing of aqueous contents. *Eur. Biophys. J.* 17:121–129.

Kozlov, M. M., and V. S. Markin. 1983. Possible mechanism of membrane fusion. *Biofizika.* 28:255–261.

Kozlov, M. M., and M. Winterhalter. 1991. Elastic moduli and neutral surface for strongly curved monolayers: analysis of experimental results. *J. Phys. II France.* 1:1085–1100.

Kozlovsky, Y., and M. Kozlov. 2002. Stalk model of membrane fusion: solution of energy crisis. *Biophys. J.* 88:882–895.

Kuzmin, P. I., J. Zimmerberg, Y. A. Chizmadzhev, and F. S. Cohen. 2001. A quantitative model for membrane fusion based on low-energy intermediates. *Proc. Natl. Acad. Sci. U.S.A.* 98:7235–7240.

Lang, T., D. Bruns, D. Wenzel, D. Riedel, P. Holroyd, C. Thiele, and R. Jahn. 2001. SNAREs are concentrated in cholesterol-dependent clusters that define docking and fusion sites for exocytosis. *EMBO J.* 20: 2202–2213.

Laradji, M., A. C. Shi, J. Noolandi, and R. C. Desai. 1997. Stability of ordered phases in diblock copolymer melts. *Macromolecules.* 30: 3242–3255.

Lee, J., and B. R. Lentz. 1997. Evolution of lipidic structures during model membrane fusion and the relation of this process to cell membrane fusion. *Biochemistry.* 36:6251–6259.

Leikin, S., M. M. Kozlov, N. L. Fuller, and R. P. Rand. 1996. Measured effects of diacylglycerol on structural and elastic properties of phospholipid membranes. *Biophys. J.* 71:2623–2632.

Leikin, S. L., M. M. Kozlov, L. V. Chernomordik, V. S. Markin, and Y. A. Chizmadzhev. 1987. Membrane fusion: overcoming of the hydration barrier and local restructuring. *J. Theor. Biol.* 129:411–425.

Li, X. J., and M. Schick. 2000. Fluctuations in mixtures of lamellar- and nonlamellar-forming lipids. *J. Chem. Phys.* 112:10599–10607.

Lieber, M. R., and T. L. Steck. 1989. Hemolytic holes in human erythrocyte membrane ghosts. *Methods Enzymol.* 173:356–367.

Lindau, M., and W. Almers. 1995. Structure and function of fusion pores in exocytosis and ectoplasmic membrane fusion. *Curr. Opin. Cell Biol.* 7:509–517.

Luzzati, V. 1968. X-Ray Diffraction Studies of Lipid-Water Systems. *In* Biological Membranes. D. Chapman, editor. Academic Press, New York, 71–123.

Markin, V., and J. Albanesi. 2002. Membrane fusion: stalk model revisited. *Biophys. J.* 82:693–712.

Markin, V. S., M. M. Kozlov, and V. L. Borovjagin. 1984. On the theory of membrane fusion: the stalk mechanism. *Gen. Physiol. Biophys.* 3:361–377.

May, S. 2000. Protein-induced bilayer deformations: the lipid tilt degree of freedom. *Eur. Biophys. J. Biophys. Lett.* 29:17–28.

May, S., and A. Ben-Shaul. 1999. Molecular theory of lipid-protein interaction and the Lalpha-HII transition. *Biophys. J.* 76:751–767.

Melikyan, G. B., S. A. Brener, D. C. Ok, and F. S. Cohen. 1997. Inner but not outer membrane leaflets control the transition from glycosylphosphatidylinositol-anchored influenza hemagglutinin-induced hemifusion to full fusion. *J. Cell Biol.* 136:995–1005.

Melikyan, G. B., J. M. White, and F. S. Cohen. 1995. GPI-anchored influenza hemagglutinin induces hemifusion to both red blood cell and planar bilayer membranes. *J. Cell Biol.* 131:679–691.

Monck, J. R., and J. M. Fernandez. 1992. The exocytotic fusion pore. *J. Cell Biol.* 119:1395–1404.

Muller, M., K. Katsov, and M. Schick. 2002. New mechanism of membrane fusion. *J. Chem. Phys.* 116:2342–2345.

Needham, D., and R. M. Hochmuth. 1989. Electro-mechanical permeabilization of lipid vesicles: role of membrane tension and compressibility. *Biophys. J.* 55:1001–1009.

Niggemann, G., M. Kummrow, and W. Helfrich. 1995. The bending rigidity of phosphatidylcholine bilayers: dependence on experimental methods, sample cell sealing and temperature. *J. Phys. II.* 5:413–425.

Nitsche, J. C. C. 1989. Lectures on Minimal Surfaces. University Press, Cambridge.

Noguchi, H., and M. Takasu. 2001a. Fusion pathways of vesicles: a Brownian dynamics simulations. *J. Chem. Phys.* 115:9547–9551.

Noguchi, H., and M. Takasu. 2001b. Self-assembly of amphiphiles into vesicles: a Brownian dynamics simulation. *Phys. Rev. E.* 64:art no 041913.

Olbricht, K. 1984. Synchronous exocytosis in Paramecium cells: II. Intramembranous changes analysed by freeze-fracturing. *Exp. Cell Res.* 151:14–20.

Ornberg, R. L., and T. S. Reese. 1981. Beginning of exocytosis captured by rapid-freezing of Limulus amebocytes. *J. Cell Biol.* 90:40–54.

Pantazatos, D. P., and R. C. MacDonald. 1999. Directly observed membrane fusion between oppositely charged phospholipid bilayers. *J. Membr. Biol.* 170:27–38.

Peters, C., M. J. Bayer, S. Buhler, J. S. Andersen, M. Mann, and A. Mayer. 2001. Transcomplex formation by proteolipid channels in the terminal phase of membrane fusion. *Nature.* 409:581–588.

Rand, R. P., and N. L. Fuller. 1994. Structural dimensions and their changes in a reentrant hexagonal-lamellar transition of phospholipids. *Biophys. J.* 66:2127–2138.

Rand, R. P., and V. A. Parsegian. 1989. Hydration forces between phospholipid bilayers. *Biochim. Biophys. Acta.* 988:351–376.

Siegel, D. P. 1993. Energetics of intermediates in membrane fusion: comparison of stalk and inverted micellar intermediate mechanisms. *Biophys. J.* 65:2124–2140.

Siegel, D. P. 1999. The modified stalk mechanism of lamellar/inverted phase transitions and its implications for membrane fusion. *Biophys. J.* 76:291–313.

Siegel, D. P., J. L. Burns, M. H. Chestnut, and Y. Talmon. 1989. Intermediates in membrane fusion and bilayer/nonbilayer phase transitions imaged by time-resolved cryo-transmission electron microscopy. *Biophys. J.* 56:161–169.

Siegel, D. P., and R. M. Epand. 1997. The mechanism of lamellar-to-inverted hexagonal phase transitions in phosphatidylethanolamine: implications for membrane fusion mechanisms. *Biophys. J.* 73: 3089–3111.

Siegel, D. P., W. J. Green, and Y. Talmon. 1994. The mechanism of lamellar-to-inverted hexagonal phase transitions: a study using temperature-jump cryo-electron microscopy. *Biophys. J.* 66:402–414.

Skehel, J. J., and D. C. Wiley. 2000. Receptor binding and membrane fusion in virus entry: the influenza hemagglutinin. *Annu. Rev. Biochem.* 69:531–569.

Song, L. Y., Q. F. Ahkong, D. Georgescauld, and J. A. Lucy. 1991. Membrane fusion without cytoplasmic fusion (hemi-fusion) in erythrocytes that are subjected to electrical breakdown. *Biochim. Biophys. Acta.* 1065:54–62.

Szleifer, I., D. Kramer, A. Ben-Shaul, W. M. Gelbart, and S. A. Safran. 1990. Molecular theory of curvature elasticity in surfactant films. *J. Chem. Phys.* 92:6800–6817.

Taupin, C. 1975. Osmotic pressure induced pores in phospholipid vesicles. *Biochemistry.* 14:4771–4775.

Walter, A., P. L. Yeagle, and D. P. Siegel. 1994. Diacylglycerol and hexadecane increase divalent cation-induced lipid mixing rates between phosphatidylserine large unilamellar vesicles. *Biophys. J.* 66: 366–376.

Weaver, J., and Y. Chizmadzhev. 1996. Theory of electroporation: a review. *Bioelectrochem. Bioenerg.* 41:135–160.

Zimmerberg, J., F. S. Cohen, and A. Finkelstein. 1980. Fusion of phospholipid vesicles with planar phospholipid bilayer membranes: I. Discharge of vesicular contents across the planar membrane. *J. Gen. Physiol.* 75:241–250.